

Supplementary Table 1 Data collection and refinement statistics

	MR1
Data collection	
Space group	$P2_12_12_1$
Cell dimensions	
<i>a</i> , <i>b</i> , <i>c</i> (Å)	59.15, 89.78, 171.34
α , β , γ (°)	90, 90, 90
Resolution (Å)	89.78-3.2 (3.37-3.2) *
R_{merge}	26.6 (68.6)
R_{pim}	16.6 (42.5)
$I/\sigma I$	4.5 (1.8)
Completeness (%)	98.1 (95.7)
Redundancy	3.4 (3.4)
Refinement	
Resolution (Å)	3.2
No. reflections	15334
$R_{\text{work}}/ R_{\text{free}}$	19.6/25.8
No. atoms	
Protein	5762
6-formyl pterin	27
Phosphate	5
Chlorine	1
B-factors	
Protein	38.7
6-formyl pterin	46
R.m.s deviations	
Bond lengths (Å)	0.010
Bond angles (°)	1.16

*Highest resolution shell is shown in parenthesis.

Data was collected from a single crystal.

$$^1 R_{\text{p.i.m}} = \frac{\sum_{\text{hkl}} [1/(N-1)]^{1/2} \sum_i |I_{\text{hkl},i} - \langle I_{\text{hkl}} \rangle|}{\sum_{\text{hkl}} \langle I_{\text{hkl}} \rangle}$$

$$^2 R_{\text{factor}} = \frac{(\sum | |F_o| - |F_c| |)}{(\sum |F_o|)} - \text{for all data except as indicated in footnote 3.}$$

³ 5% of data was used for the R_{free} calculation

Values in parentheses refer to the highest resolution bin.

Supplementary Table 2. Contacts between MR1 and 6-formyl-pterin

6-formyl pterin	MR1	Bond
C9	Lys43 ^{NZ}	Covalent link
	Lys43 ^{CD}	VDW
	Lys43 ^{CE}	VDW
	Tyr7 ^{CD1}	VDW
	Tyr7 ^{CE1}	VDW
	Tyr7 ^{CZ}	VDW
C6	Lys43 ^{NZ}	VDW
	Lys43 ^{CE}	VDW
	Tyr7 ^{CD1}	VDW
	Tyr7 ^{CE1}	VDW
	Tyr7 ^{CZ}	VDW
N5	Lys43 ^{NZ}	VDW
	Tyr7 ^{CG}	VDW
	Tyr7 ^{CD1}	VDW
C4A	Trp69 ^{CZ3}	VDW
C4	Arg9 ^{NH2}	VDW
	Trp69 ^{CZ3}	VDW
	Arg94 ^{NH1}	VDW
	Ile96 ^{CD1}	VDW
O4	Arg9 ^{NH2}	VDW
	Trp69 ^{CZ3}	VDW
	Arg94 ^{NH1}	VDW
	Arg9 ^{NE}	VDW
	Tyr7 ^{CB}	VDW
N3	Arg9 ^{NH2}	VDW
	Trp69 ^{CZ3}	VDW
	Arg94 ^{NH1}	H-bond
	Ile96 ^{CG1}	VDW
	Ile96 ^{CD1}	VDW
C2	Arg94 ^{NH1}	VDW
	Ile96 ^{CD1}	VDW
N2	Arg94 ^{NH1}	VDW
	Ile96 ^{CD1}	VDW
	Gln153 ^{OE1}	VDW
N8	Tyr62 ^{CZ}	VDW
	Tyr62 ^{CE1}	VDW
	Tyr62 ^{OH}	VDW
C7	Tyr62 ^{CZ}	VDW
	Lys43 ^{NZ}	VDW
	Tyr62 ^{CD1}	VDW
	Tyr62 ^{CE1}	VDW
	Tyr7 ^{CZ}	VDW

- Atomic contacts determined using the CCP4i implementation of *CONTACT* and a cutoff of 4.0 Å for vdw interactions and 3.3 Å for h-bond interactions.

Supplementary Table 3

This table highlights the MAIT activating strains of bacteria/yeast and non-activating strains of bacteria as defined by Le Bourhis et al and Gold et al 2010. In the context of MAIT activation, a defining distinction between the activating/non-activating strains is that (with the possible exception of *L. acidophilus*; note that some ambiguity pertains to the nomenclature and thus presence/absence of the riboflavin metabolic pathway of *Lactobacillus* species [www.atcc.org/]) the former possess the riboflavin metabolic pathway whereas the latter do not.

Activating Strains of bacteria:

Escherichia coli
 Pseudomonas aeruginosa
 Klebsiella pneumoniae
 * Lactobacillus acidophilus
 Staphylococcus aureus
 Staphylococcus epidermidis
 Mycobacterium abscessus
 Mycobacterium tuberculosis
 Salmonella typhimurium

Non-activating Strains of bacteria:

Streptococcus group A
 Enterococcus faecalis
 Listeria monocytogenes

Activating Strains of yeast:

Candida albicans
 Candida glabrata
 Saccharomyces cerevisiae
 Please see

<http://www.genome.jp/kegg/pathway/map/map00740.html>

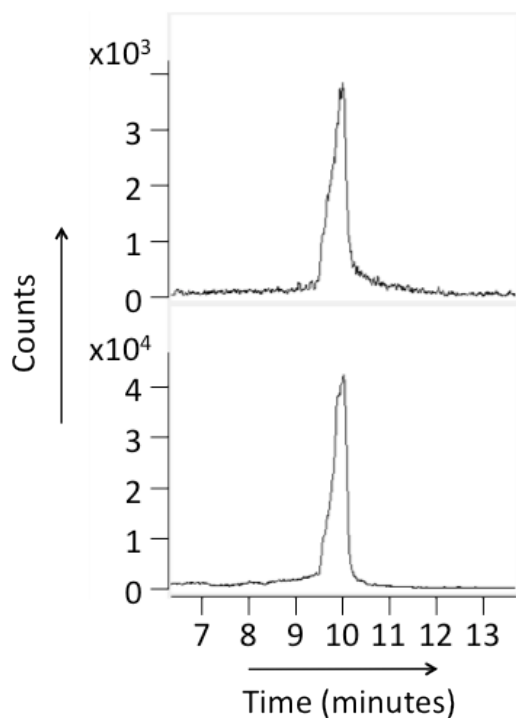
for the KEGG Riboflavin Metabolic Pathway

References:

Le Bourhis et al. 2010
 Gold et al. 2010

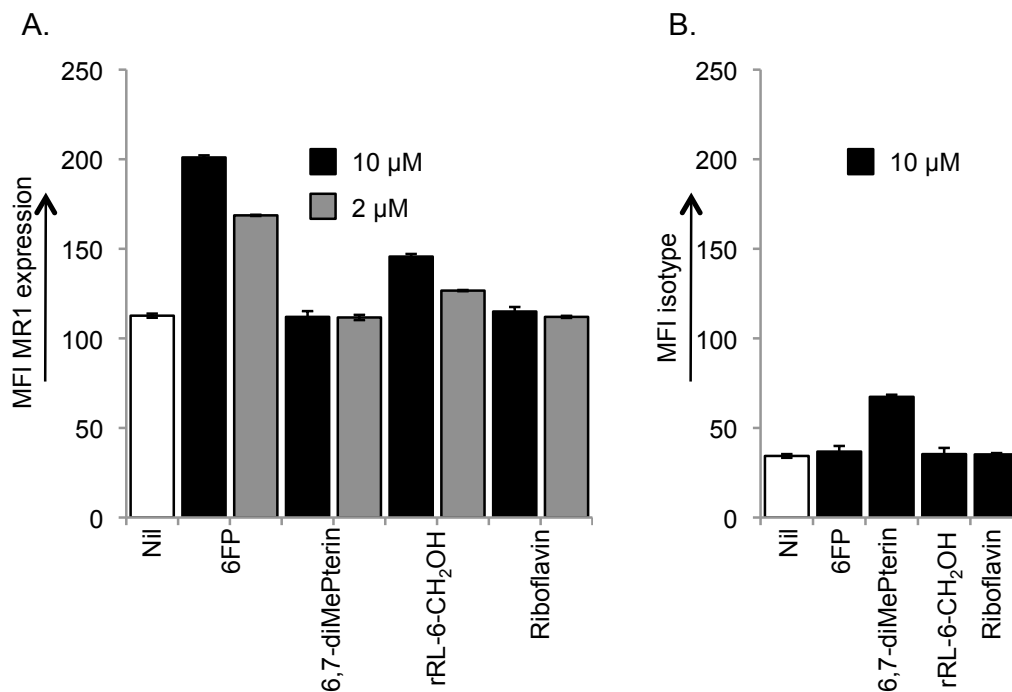
For the organisms identified as MAIT activating (12) and non-activating (3), analysis of these categorical data using the Fisher's exact test yields a two-tailed P value of 0.0022.

* A Fishers exact test on all organisms excluding *L. acidophilus* (as the riboflavin pathway is uncertain in the strain of *L. acidophilus*) yields a two-tailed p value of 0.0027.

Supplementary Figure 1. Mass spectrometry analysis of MR1 refolded with 6-FP.

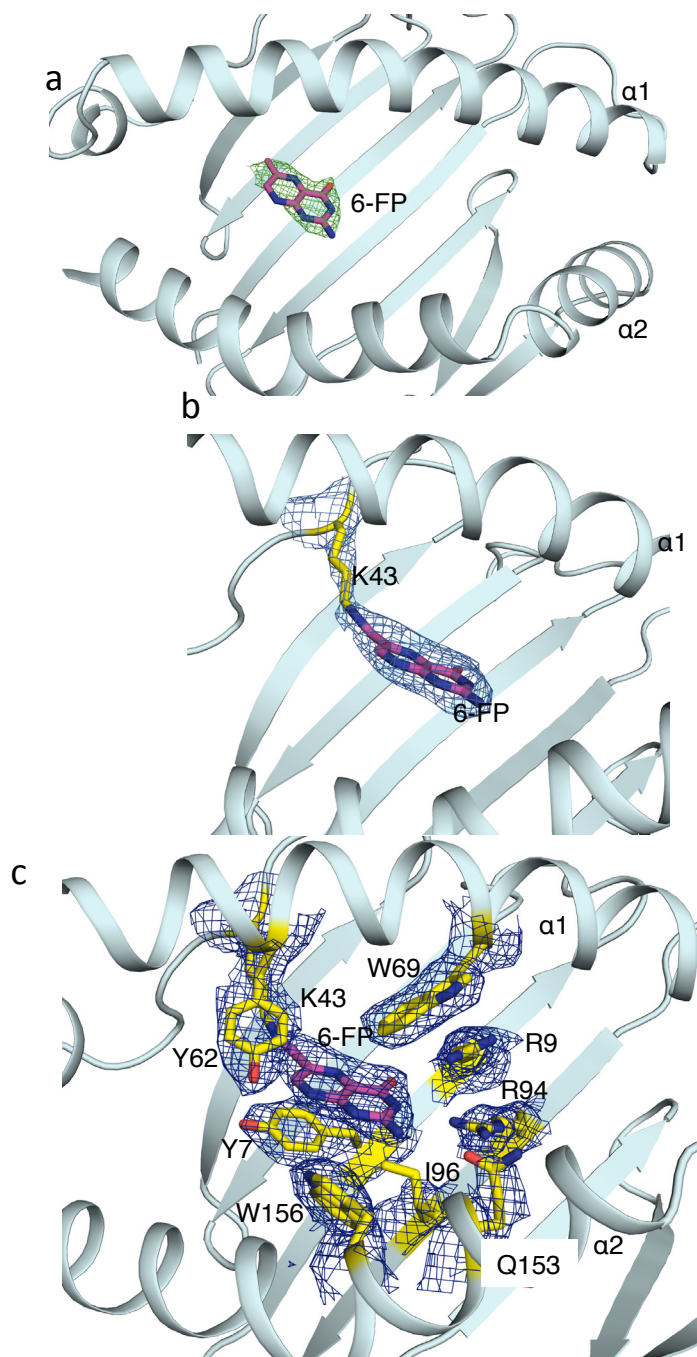
Shown are extracted ion chromatograms (EIC) of 190.0347 for 6-formyl pterin refolded with MR1 (upper panel) and 6-formyl pterin (190.0328) (lower panel), with counts on the Y-axis versus time on the X-axis. Background counts were obtained with EIC from control buffer-only samples (not shown).

Supplementary Figure 2. Increase of MR1 surface expression by stimulatory and non-stimulatory MR1 ligands.



C1R cells (10^5 /well in 200μl RF-10) were incubated for 4 hr at 37°C with compounds at 10 and 2 μM final concentration. **A.** MR1 expression was analysed by flow cytometry using the MR1-specific Ab 26.5 and **B.** compared to an isotype control 8A5 at 10 μg/ml followed by PE-conjugated goat-anti-mIgG (BD Pharmingen). Graphs show MFI of PE fluorescence, expressed as mean +/- SEM from triplicate samples.

Supplementary Figure 3

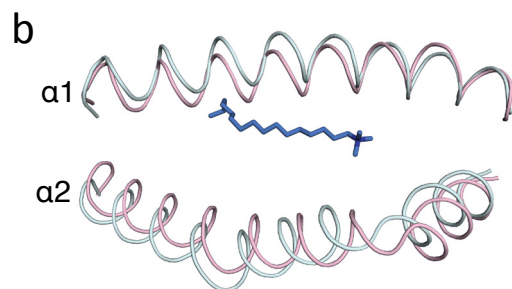


a) omit map of 6-FP contoured at 2.5σ . b) final 2Fo-Fc map of 6-FP and Lys43 of MR1 contoured at 0.8σ . c) final 2Fo-Fc map of MR1 residues that contact 6-FP contoured at 1.0σ .

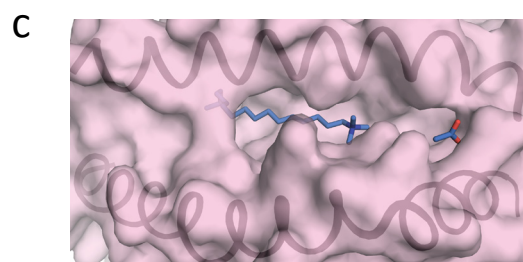
Supplementary Figure 4. Sequence and structural comparison of MR1 and avian MHC

a

MR1	RTHSLRYFRLGVSDPIHGVPFISVGYVDSHPITTYDSVTRQKEPRAPWMAENLAPDHW	60
avian_MHC	GSHSLRYFLTGMTDPGPGMPRFVIVGYVDDKIFGTYNKSRTAQPIVEMLPQ-EDQEHWD	59
	***** * ** * * * ***** ** * * *	**
MR1	RYTQLLRGWQQMFVKVELKRLQRHYNHS-GSHTYQRMIGCELLEDGSTTGFLQYAYDGQDF	119
avian_MHC	TQTQKAQGGERDFDWNLNRLPERYNKSKGSHTMOMMFGCDILEDGSIIRGYDQYAFDGRDF	119
	** * * * * ** * * * * * ** * * * * *	** ** * * *
MR1	LIFNKDTLSWLAVDNVAHTIKQAWEANQHELLYQKNWLEEECIAWLKRFLFYGKDTLQRT	179
avian_MHC	LAFDMDTMTFTAADPVAEITKRRWETEGTYAERWKHELGTVCVQNLRRYLEHGKAALKRR	179
	* * ** * * * * * * * * * * * * * * * *	** * * * * *
MR1	EPPLVRVNRKETFPGVTFALFCKAHGFYPPEIYMTWMKNGEEIVQEIDYGDILPSGDGTYQ	239
avian_MHC	VQPEVRVWGKEAD-GILTLSCHAHGFYPRPITISWMKDGMRDQETRWGGIVPNSDGYTH	238
	* ** * * * * * * * * * * * * * * * *	** * * * * *
MR1	AWASIELDPQSSNLYSCHVEHSGVHMLQVP----	270
avian_MHC	ASAAIDVLPEDGDKYWCVEHASLPQPLFSWEPQ	273
	* * * * * * * * * * * * * * * *	** * * * *

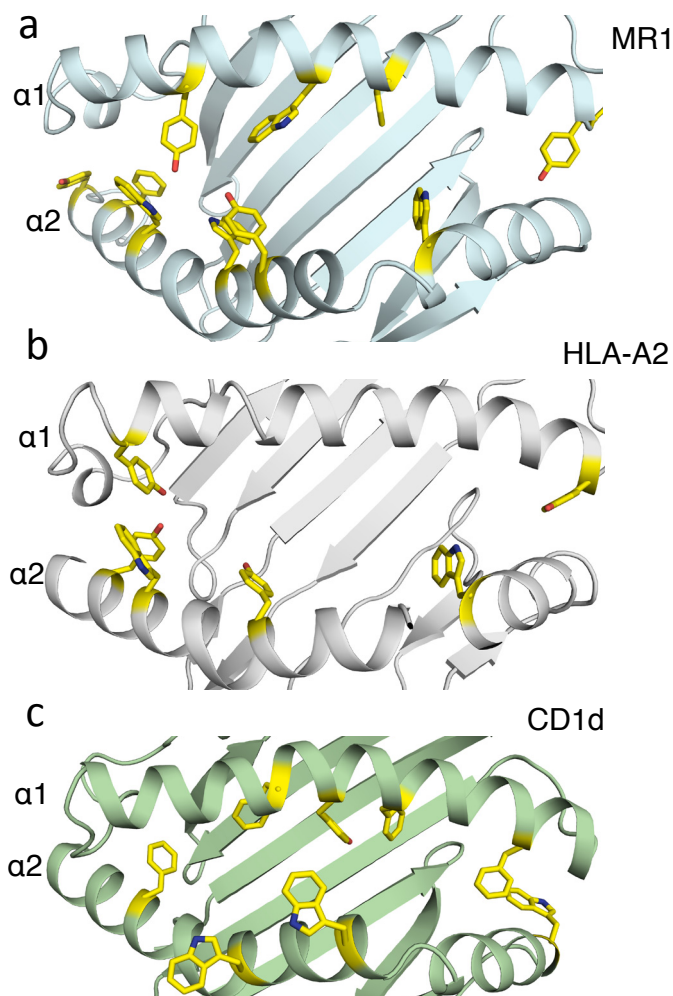


Pink= avian MHC bound to a surfactant
Cyan= MR1

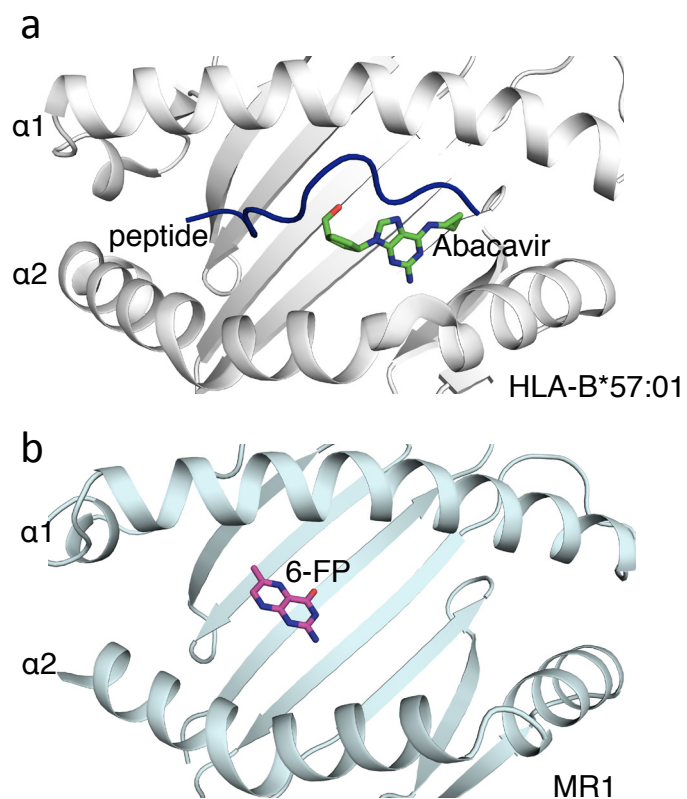


Surface representation of avian MHC bound to a surfactant

a) Sequence alignment of MR1 with avian MHC. Identical residues are shown as *. b) overlay of $\alpha 1$ and $\alpha 2$ helices using the residues within the antigen binding cleft of MR1 with avian MHC (PDB code 3P73) and c) surface presentation of avian MHC bound to a surfactant. MR1, cyan; avian MHC, pink; surfactant, blue sticks.

Supplementary Figure 5. Comparison of Ag-binding clefts of MR1, HLA-A2 and CD1d

Antigen binding cleft of MR1 (a), HLA-A2 (b) and CD1d (c) showing aromatic residues in yellow on the $\alpha 1$ and $\alpha 2$ helices.



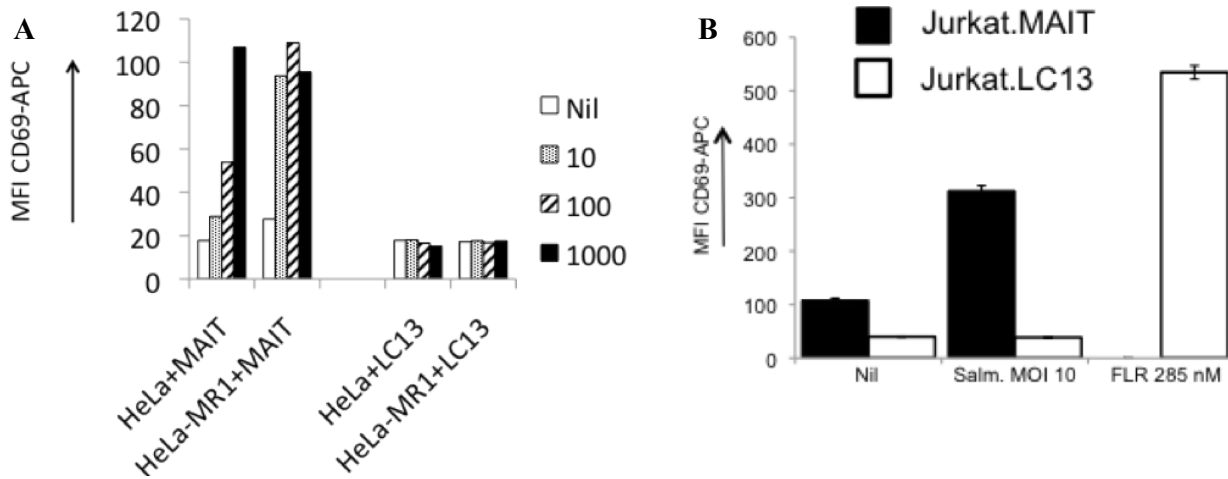
Supplementary Figure 6. Comparison of how 6-FP binds MR1 and abacavir binds HLA B*57:01

a) antigen binding cleft of HLA-B*57:01 bound to abacavir. b) antigen binding cleft of MR1 bound to 6-FP. HLA-B*57:01, grey; peptide, blue; abacavir, green; MR1, cyan; 6-FP, magenta.

Supplementary Figure 7. Sequence alignment of MR1 from different species

human	RTHSLRYFRLGVSDPIHGVPFISVGYVDSHPITTYDSVTRQKEPRAPWMAENLAPDHW	60
chimpanzee	RTHSLRYFRLGVSDPIHGVPFISVGYVDSHPITTYDSVTRQKEPRAPWMAENLAPDHW	60
orangutan	RTHSLRYFRLGVSDPIRGVPEFISVGYVDSHPITTYDSVTRQKEPRAPWMAENLAPDHW	60
sheep	RTHSLRYFRLGISSEPGYGIPEFISAGYVDSHPITMYSVSQLKEPRAPWMAENLEPDHW	60
bovine	RTHSLRYFRLGISSEPGYGIPEFISAGYVDSHPITMYSVSQLKEPRALWMEENLAPDHW	60
pig	-THSLRYFRLGISDPGHEMPEFISVGYVDSYPITTYDSVSRQKEPRAPWMAENLEPDHW	59
rat	RTHSLRYFRLAISDPGPGVPEFISVGYVDSHPITTYDSVTRQKEPRAPWMAENLAPDHW	60
mouse	RTHSLRYFRLAVSDPGVVPFISVGYVDSHPITTYDSVTRQKEPKAPWMAENLAPDHW	60
Tasmanian devil	RTHSLRYFRLGVSDSTQGIPEFISVGYVDSHPITSYDSIRRQKMPQASWMEENLGS	60
opossum	-THSLRYFRLGLSDSNQGMPEFISVGYVDSHPITSYDSNGRQKMPQASWMEENLGS	59
	***** * ***** ** * * * * * * * * * * * * * * * * * *	
human	RYTQLLRGWQMFKVELKRLQRHYNHSG-SHTYQRMIGCELLEDGSTTGFLQYAYDGQDF	119
chimpanzee	RYTQLLRGWQMFKVELKRLQRHYNHSG-SHTYQRMIGCELLEDGSTTGFLQYAYDGQDF	119
orangutan	RYTQLLRGWQMFKVELKRLQRHYNHSG-SHTYQRMIGCELLEDGSTTGFLQYAYDGQDF	119
sheep	RYTQLLRGWQAFKVELKQLQHYNHSG-FNTYQRMIGCELLEDGSTTGFLQYAYDGQDF	119
bovine	RYTQLLRGWQAFKVELKQLQHYNHSG-FHTYQRMIGCELLEDGSTITGFLQYAYDGQDF	119
pig	RYTQLLRGWQTFKAEKQLQRHYNHSG-LHTYQRMIGCELLEDGSTTGFLQYAYDGQDF	118
rat	RYTQLLRGWQRTFQTELRLQRHYNHSG-LHTYQRMIGCELLEDGSTTGFLQYAYDGQDF	119
mouse	RYTQLLRGWQTFKAEKRLQRHYNHSG-LHTYQRMIGCELLEDGSTTGFLQYAYDGQDF	119
Tasmanian devil	KYTQLLRGWQTFKTELRLQNHYNHSGFHTYQRMIGCELLEDGSTTGFLQYAYDGKDF	120
opossum	KYTQLLRGWQTFKIELRALQNHYNHSGFHIYQRMIGCELLEDGSTTGFLQYAYDGKDF	119
	***** *	
human	LIFNKDTLSWLAVDNVAHTIKQAEWANQHELLYQKNWLEEECIAWLKRFLEYGKDTLQRT	179
chimpanzee	LIFNKDTLSWLAVDNVAHTIKQAEWANQHELLYQKNWLEEECIAWLKRFLEYGKDILQRT	179
orangutan	LIFNKDTLSWLAVDNVAHTIKRAEWAHQHELLYQKNWLEEECIAWLKRFLEYGKDTLQRT	179
sheep	LIFNKDTLSWIAMDNVANIIRRAEWAHRHELQYQKNWLEEECIAWLKRFLEYGKDTLQRT	179
bovine	LIFNKDTLSWAMDNVADIIRRVWEANRHELQYQKNWLEEECIAWLKRFLEYGKDALQRT	179
pig	LIFNKDTLSWMAVDNVAHITKQAEWANWHELQYQKNWLEEECIAWLRRFLEYGKDTLQRT	178
rat	IVFDKDTLSWLAMDVAHITKRAEWAHLHELQYQKNWLEEECIAWLKRFLEYGSDALERT	179
mouse	LIFNKDTLSWLAMDVAHITKQAEWANLHELQYQKNWLEEECIAWLKRFLEYGRDTLERT	179
Tasmanian devil	LIFDKDLSWIAVDNVARLTKQVWETNLNELRYQKNWLETECIAWLKKFLDFGKDSFQRT	180
opossum	IVFNKESLSWIAMDVARLTKQAEWANRNLRYQKNWLETECIAWLKKFLDFGKDTLQRT	179
	* *	
human	EPPLVRVNRKETFPGVTLFCKAHGFYPPEIYMTWMKNGEEIVQEIYDYGDIILPSGDGTQY	239
chimpanzee	EPPLVRVNRKETFPGVTLFCKAHGFYPPEIYMTWMKNGEEIVQEIYDYGDIILPSGDGTQY	239
orangutan	EPPLVRVNRKETFPGVTLFCKAHGFYPPEIYMTWMKNGEEIVQEMDYDGIILPSGDGTQY	239
sheep	EPPKVRVNYKETFPGITTLTYCRAHGFYPPEISINWMKNGEEVVDQTNYGDIILPSGDGTQY	239
bovine	EPPKVRVNHKETFPGITTLTYCRAHGFYPPEISINWMKNGEEIFQDQDYGGIILPSGDGTQY	239
pig	EPPLVRVYHKETVPGITTLTYCRAHGFYPPEISMTWMKNEEEMVQEMDYDGIILPSGDGTQY	238
rat	EHPVVRTTRKETFPGITTLTYCRAHGFYPPEISMIWKNGEEIVQEVYDYGVLPSGDGTQY	239
mouse	EHPVVRTTRKETFPGITTLTYCRAHGFYPPEISMTWMKNGEEIAQEVYDYGVLPSGDGTQY	239
Tasmanian devil	ENPLLRGSKKSSLGITTLICRAYGFYPPEITMTWIKNGELIQEIEYDGIILPSGDGTQY	240
opossum	ETPLLRGSKKSSGITTLICRAYGFYPPEITMTWIKNGELITQIEIYDGIILPSGDGTQY	239
	* *	
human	AWASIELDPQSSNLYSCHVEHCGVHMLQVPQ	271
chimpanzee	TWASVELDPQSSNLYSCHVEHCGVHMLQVPQ	271
orangutan	TWASVELDPQSSNLYSCHVEHCGVHMLQVPQ	271
sheep	TWVSVELDSQNGDIYSCHVEHGGVHMLPGFQ	271
bovine	TWVSVELDPQNGDIYSCHVEHGGVHMLQGFQ	271
pig	TWVSVELDSQSSDVYSCHVKHCGVHTVLQGAR	270
rat	MWVSVDLDPQTKDIYSCHVEHCLQMVLEAPQ	271
mouse	TWLSVNLDPQSNVYSCHVEHCGRQMVLEAPR	271
Tasmanian devil	TWISIEIDPQSKDHYFCQVEHNDFLKVLHVP	272
opossum	TWVSIDIDPQSKDHYSCQVEHNNFLKVLHVP	271
	* *	

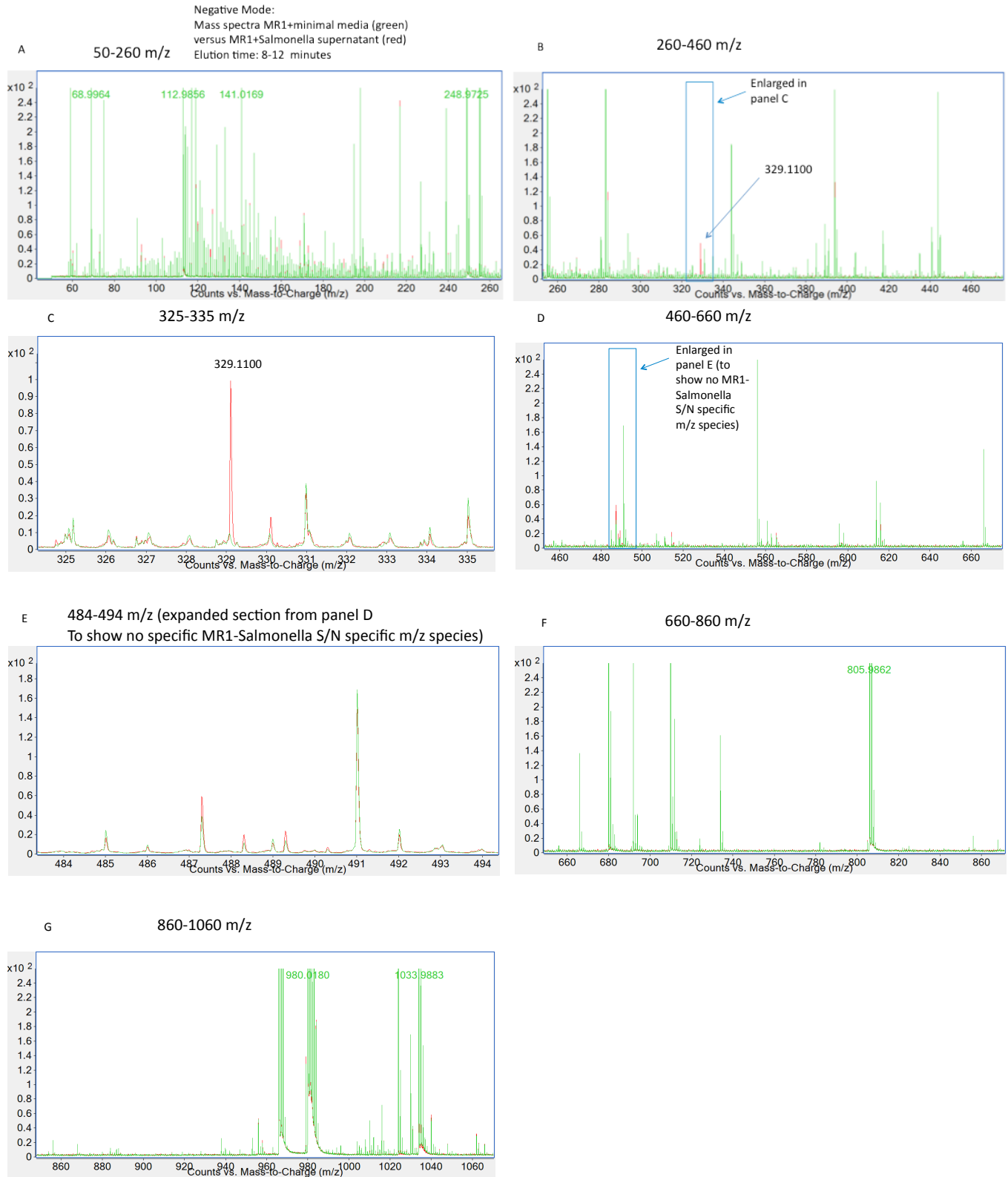
Sequence alignment of MR1 from various species. Identical residues are shown as *. Residues that contact 6-FP are conserved in all species and are highlighted in yellow.

Supplementary Figure 8. Specific activation of Jurkat.MAITs by APCs infected with *Salmonella*.

(A) HeLa antigen presenting cells infected by *Salmonella* fail to activate Jurkat cells expressing an Epstein-Barr virus-specific TCR. HeLa cells, or HeLa cells transduced with MR1 (HeLa-MR1) were either not infected (open bars), or were infected with *Salmonella typhimurium* at a multiplicity of infection of 10 (stippled bars), 100 (hatched bars) or 1000 (black bars), following which Jurkat cells expressing either a MAIT TCR (MAIT; utilizing a TRBV6-1 β chain) or the virus-specific T cell receptor LC13 were added for 18 hours before staining for CD69 cell surface expression and analysis by flow cytometry. Shown is mean fluorescence intensity of staining (MFI CD69-APC) on the Y-axis versus cell treatment on the X-axis.

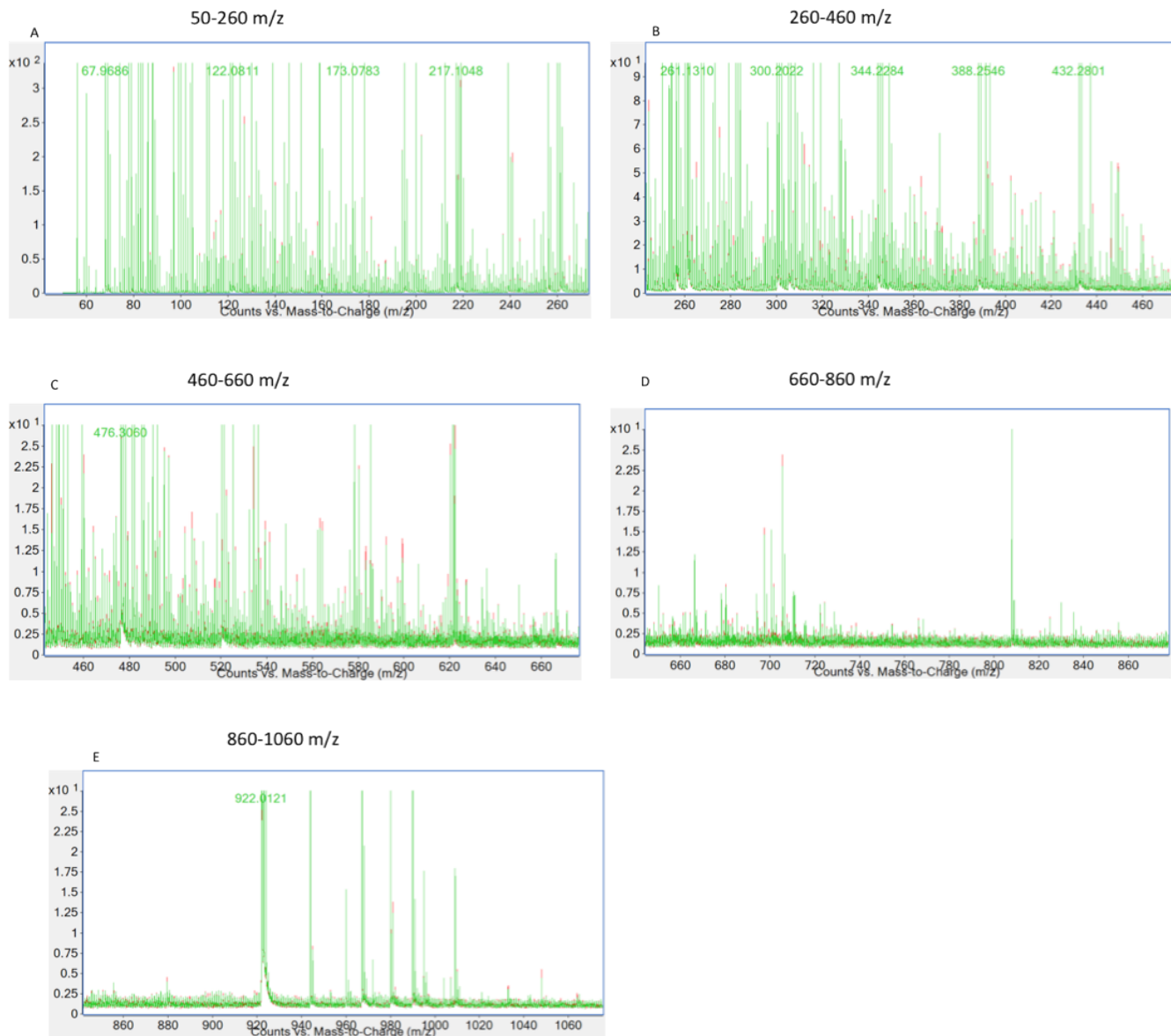
(B) C1R antigen presenting cells transduced with MR1 and infected by *Salmonella* fail to activate Jurkat cells expressing an Epstein-Barr virus-specific TCR. C1R cells transduced with MR1 were either not infected (Nil) or infected with *Salmonella typhimurium* at a multiplicity of 10 (Salm. MOI 10), following which Jurkat cells expressing either a MAIT TCR (Jurkat.MAIT; utilizing a TRBV6-1 β chain) or the virus-specific T cell receptor LC13 (Jurkat.LC13) were added for 18 hours before staining for CD69 cell surface expression and analysis by flow cytometry. Shown is mean fluorescence intensity of staining (MFI CD69-APC, expressed as mean \pm SEM from triplicate samples) on the Y-axis versus cell treatment on the X-axis. Jurkat.LC13 cells were also separately incubated with the activating Epstein-Barr virus peptide FLRGRAYGL (FLR, at 285 nM) and C1R cells expressing the restriction element HLA-B8.

Supplementary Figure 9. Negative (i) and positive (ii) ion mode data (50-1000amu)
(i)



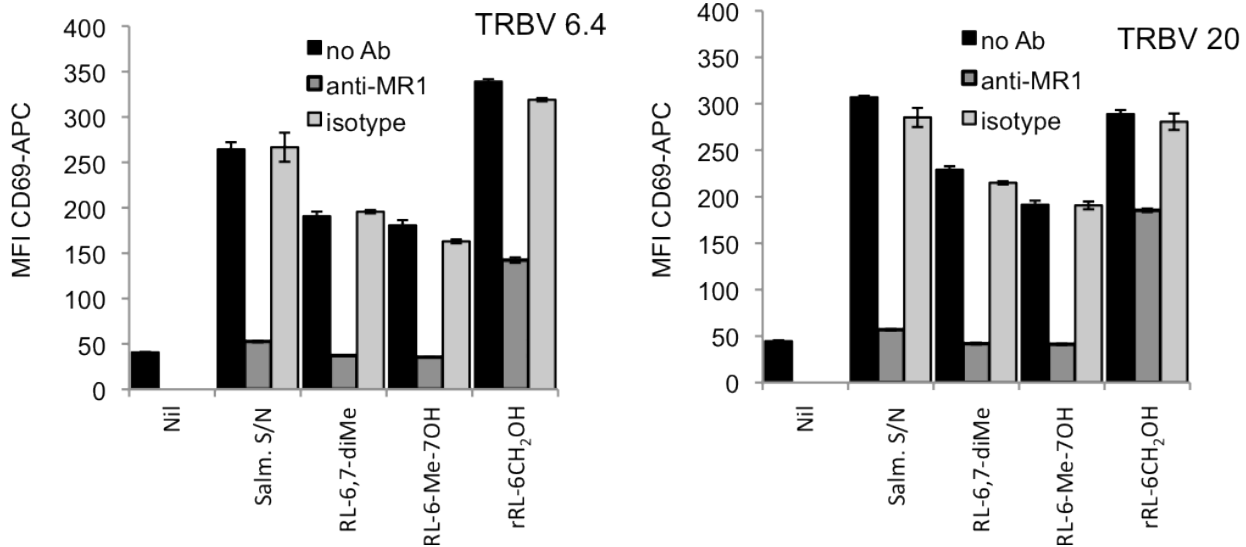
(ii)

Positive Mode:
 Mass spectra MR1+minimal media (green)
 versus MR1+*Salmonella* supernatant (red)
 Elution time: 8-12 minutes



MR1 refolded in the presence of minimal medium (green mass spectra) or in the presence of filtered supernatant from *Salmonella* cultured in the same minimal medium (red mass spectra), was loaded onto an XBridge C18 reversed phase column (Waters) and bound metabolites detected in an Agilent electrospray ionization time-of-flight (ESI TOF) mass spectrometer operating in both negative (i) or positive (ii) ion modes. Mass spectra were collected from 8-12 minutes (the 329.1100 m/z negative ion mode species has a retention time of 10.4 minutes). No m/z species unique to MR1 plus *Salmonella* supernatant were detected outside this elution time window (i.e. from 5-8 minutes and 12-16 minutes (not shown). (elution gradient performed was: 0-100% B [B: 80% acetonitrile] from 5-15 minutes) Shown in i) are mass spectra collected in negative ion mode from A) 50-260 m/z; B) 260-460 m/z; C) an expanded panel focusing on m/z from 325 to 335 to highlight the unique 329.1100 species detected with MR1 plus *Salmonella* supernatant; D) 460-660 m/z; E) an expanded panel focusing on m/z from 484 to 494 to highlight that no specific MR1 plus *Salmonella* supernatant m/z species are present within the 460-660 m/z panel; F) 660-860 m/z; and G) 860-1060 m/z. Shown in ii) are mass spectra collected in positive ion mode from A) 50-260 m/z; B) 260-460 m/z; C) 460-660 m/z; D) 660-860 m/z; and E) 860-1060 m/z.

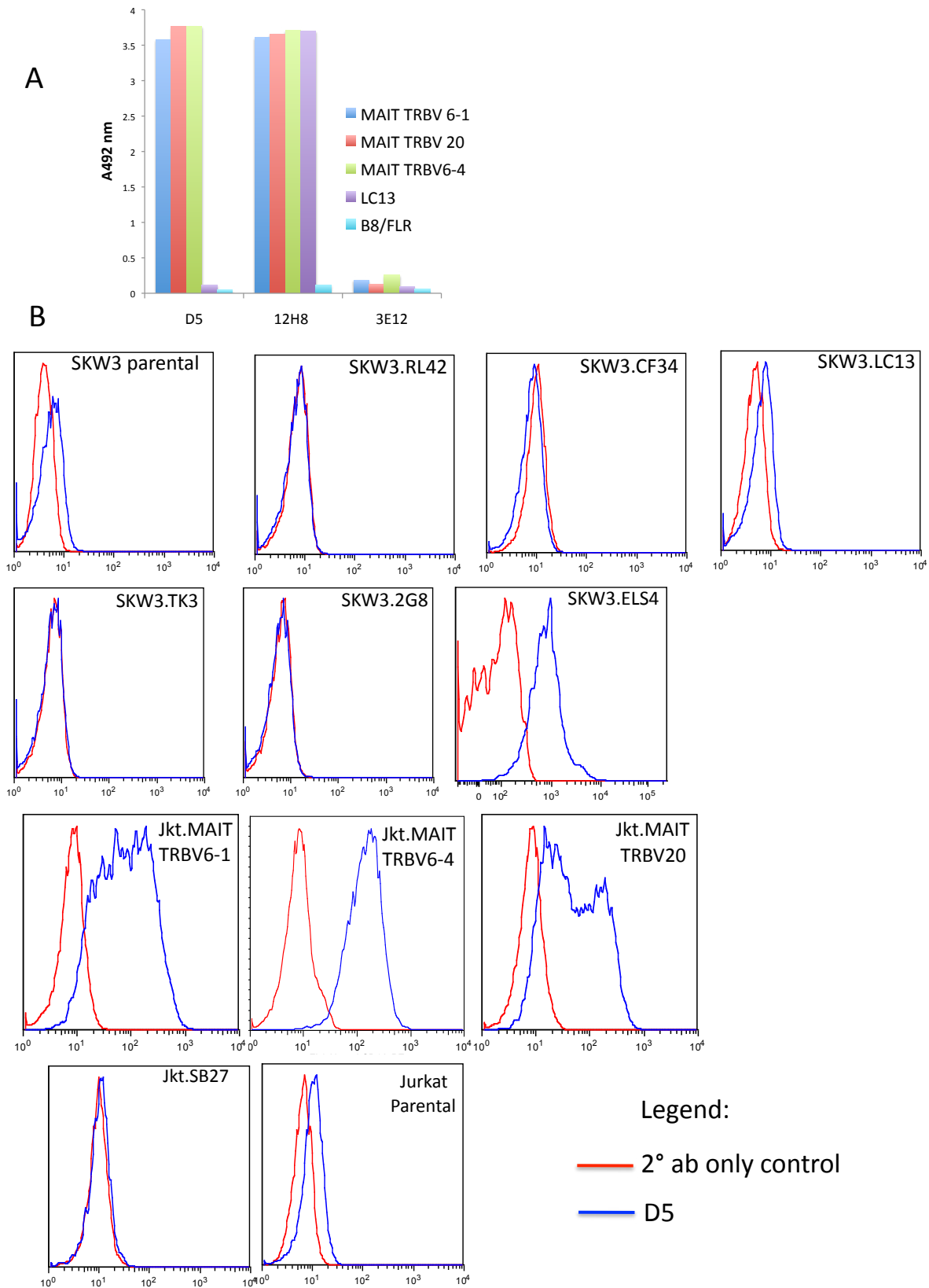
Supplementary Figure 10. Anti-MR1 blocking of Jurkat.MAIT (TRBV6.4 and TRBV20) activation by riboflavin intermediates



MR1-specific blocking of MAIT cell activation

C1R-huMR1.19 cells (10^5 /well) were preincubated with the MR1-specific Ab 26.5 ($20\mu\text{g/ml}$), isotype control W6/32 or no Ab for 2 hr. Jurkat.MAIT cells (10^5 /well) expressing the TRBV6.4 (Left hand panel) or TRBV20 MAIT TCR (Right hand panel) were added along with supernatant ($2.0\mu\text{l}$ added) or compounds (RL-6,7-diMe, RL-6-Me-7-OH, $76\mu\text{M}$ final, or rRL-6-CH₂OH: $15.2\mu\text{M}$ final) in RF-10 and incubated overnight at 37°C . CD69 expression was analysed by flow cytometry. Graph shows MFI of gated Jurkat.MAIT cells ($\text{CD}3^+$, GFP^{low}) expressed as mean \pm SEM from triplicate samples. In each case activation of MAIT cells was blocked by MR1-specific Ab 26.5, but not by the isotype control W6/32. These results were part of an experiment conducted on same day as data shown in Figure 5a,b.

Supplementary Figure 11. The D5 Mab is specific for V α 7.2 α -chain.



(A) The D5 mAb binds to soluble MAIT TCRs.

ELISA plates coated with the soluble refolded TCRs MAIT-TRBV6-1, MAIT-TRBV6-4, MAIT-TRBV20, LC13, or control HLA-B8 at 10 µg/ml were probed with the mAb D5, the TCR constant domain-reactive mAb 12H8, or a control mAb 3E12 (reactive against HLA-B57). Bound antibody was detected with a secondary HRP-conjugated anti-mouse IgG antibody and o-phenylenediamine substrate, with absorption at 492 nm shown on the Y-axis.

(B) Staining of TCR-transduced cell lines with the mAb D5.

SKW and Jurkat cells were either not transduced, or transduced with a panel of alpha and beta TCR genes encoding the T cell receptors: RL42 (Gras, JI 2012), CF34 (Gras, Immunity 2009), LC13 (Kjer-Nielsen, Immunity 2003), TK3 (Gras JEM 2010), 2G8 (Eckle, unpublished), or ELS4 (Tynan, NI 2007) (SKW cells, upper panels); or MAIT-TRBV6-1, MAIT-TRBV6-4, MAIT-TRBV20 (Reantragoon JEM 2012), or SB27 (Tynan NI 2005) (Jurkat cells, lower panels) as indicated, and stained by indirect immunofluorescence with the mAb D5 (the secondary antibody used was PE-conjugated anti-mouse IgG antibody), and subsequently analysed by flow cytometry. Shown are histogram FACS plots with intensity of staining on the X-axis. Shown below is the gene usage of the TCRs used to confirm specificity of the D5 MAb. Note that ELS4 shares the same TCR α -chain as the MAIT TCR, thereby confirming specificity of the D5 Mab for TRAV1-2 (V α 7.2)

SKW3 parental

RL42

CF34

LC13

TRAV		12-1	14	26-2
TRAJ		23	49	52
TRBV		6-2	11-2	7-8
TRBJ		2-4	2-3	2-7

TK3

2G8

ELS4

TRAV	20	5*01	1-2
TRAJ	58	29*01	6
TRBV	9	13*01	10-3*02
TRBJ	2-2	2-2*01	1-5*01

MAIT 6-1

MAIT 6-4

MAIT20

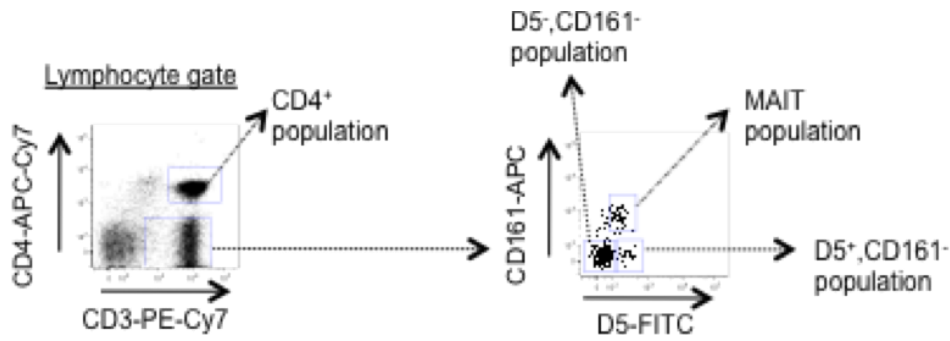
TRAV	1-2	1-2	1-2
TRAJ	33	33	33
TRBV	6-1	6-4	20-1
TRBJ	1-2	2-1	2-1

SB27

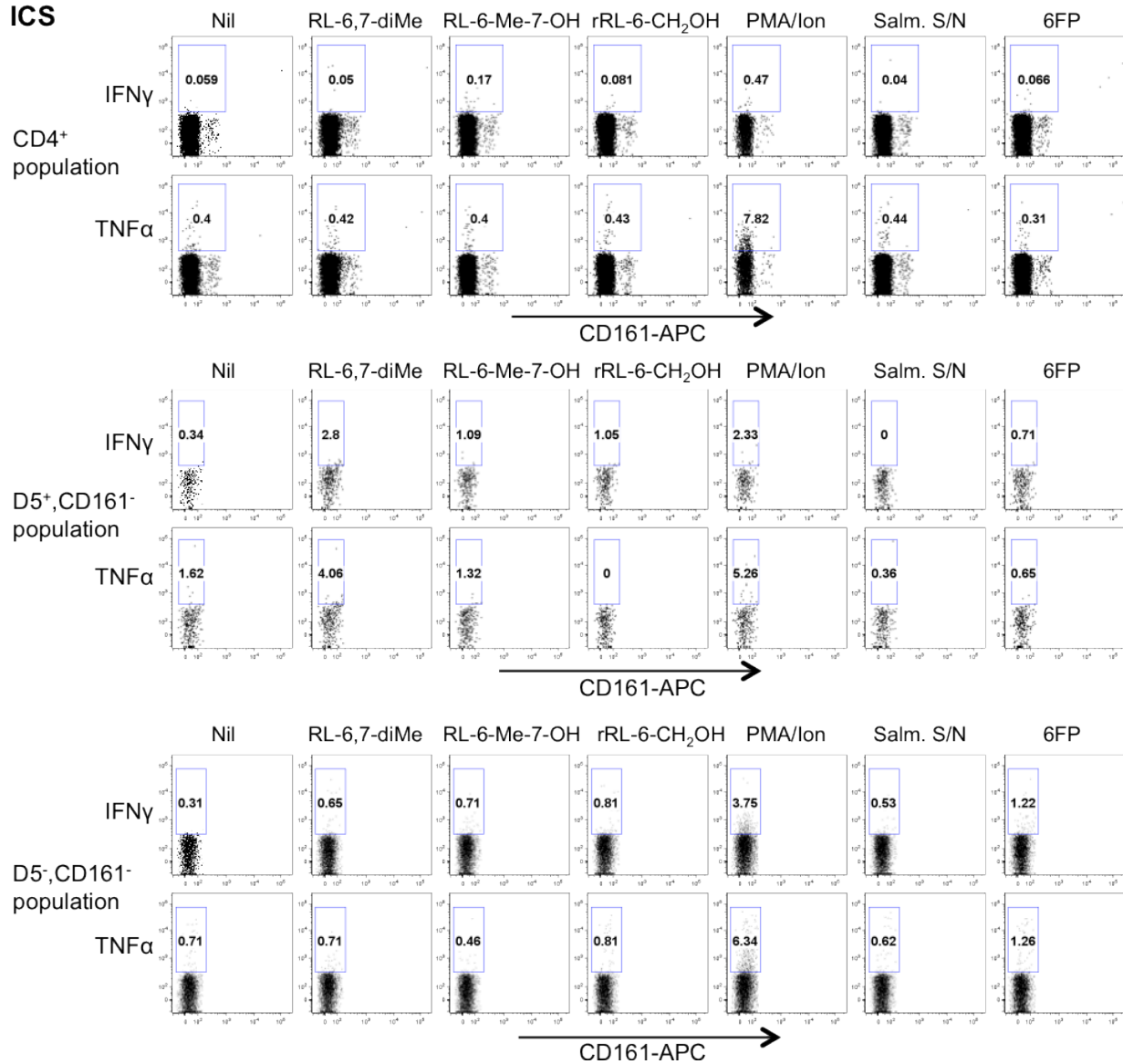
Jurkat parental

TRAV	19	
TRAJ	34	
TRBV	6-1	
TRBJ	2-7	

Supplementary Figure 12. Riboflavin metabolites, non-MAIT cells and MAIT cells



ICS



Upper panels: gating strategies for CD4⁺; D5⁺/CD161⁻; and D5⁻/CD161⁻ populations of CD3-positive lymphocytes.

Lower three sets of panels: ICS. PBMCs were mixed with C1R cells expressing MR1 (10^5 each/well) and *Salmonella* supernatant (Salm. S/N; 2 μ l); or compounds (RL-6,7-diMe, RL-6-Me-7-OH, 6-FP: 76.2 μ M final, rRL-6-CH₂OH: 0.152 μ M final); or PMA and ionomycin (PMA/Ion; 2 ng/ml and 1 ng/ml respectively) in 220 μ l RF-10 and incubated at 37 °C. After 1 hr incubation, 10 μ M brefeldin A was added and cells incubated overnight. Cells were stained for surface markers, fixed in 1% paraformaldehyde and permeabilised with 1% saponin prior to intracellular cytokine staining. Plots show gated cells from the same three non-MAIT populations with staining for IFN γ or TNF on the Y-axis versus CD161-APC staining on the X-axis for one representative sample from three.

